

Multivariate rough fractional volatility – How correlations improve forecasting and statistical inference

Markus Bibinger



joint work with Jun Yu and Chen Zhang

Conference Quantitative Finance at La Défense 2026
Nanterre

18th June 2026

Outline

- 1 Motivation and literature
- 2 Multivariate fBm and its correlation structure
- 3 Optimal forecasts for mfBm
- 4 Statistics for mfBm
- 5 Empirical analysis

Outline

- 1 Motivation and literature
- 2 Multivariate fBm and its correlation structure
- 3 Optimal forecasts for mfBm
- 4 Statistics for mfBm
- 5 Empirical analysis

Rough volatility paradigm and literature

Univariate fBm $(B_t^H)_{t \in \mathbb{R}}$ with Hurst exponent $H \in (0, 1)$ is a Gaussian process with continuous paths, $\mathbb{E}[B_t^H] = 0$, for all t , and autocovariances

$$\text{Cov}(B_{t+h}^H, B_t^H) = w(t, h, H), \text{ with } w(t, h, H) = \frac{1}{2}(|t+h|^{2H} + |t|^{2H} - |h|^{2H}).$$

For the increments $\Delta_k B^H = B_{k\Delta}^H - B_{(k-1)\Delta}^H$, $1 \leq k \leq n$:

$$\text{Cov}(\Delta_k B^H, \Delta_j B^H) = \Delta^{2H} \gamma(|k-j|),$$

with $\gamma(r) = \frac{1}{2}(|r+1|^{2H} + |r-1|^{2H} - 2|r|^{2H})$, $r \in \mathbb{Z}$.

Variants of fBm and fOU are used in three different volatility models:

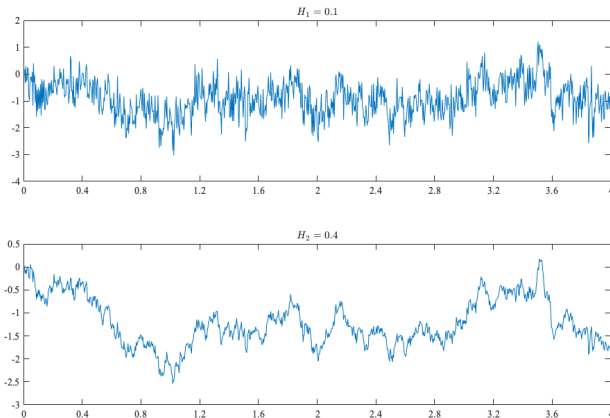
	Model	applied to	references
1	direct observations	RVs on coarse grid	Gatheral et al. (2018), Wang, Xiao & Yu (2023), ...
2	with small noise	IVs on coarse grid	Fukasawa et al. (2022), Bolko et al. (2023), ...
3	latent, price obs.	intra-day hf	Chong & Todorov (2025), Chong et al. (2024), ...

Asymptotic theory in high-frequency or low-frequency regime.

Time-space correlation patterns

Can two real-valued processes exhibit markedly different autocorrelation structures and persistence patterns while maintaining strong contemporaneous correlation?

Example: Two fBms with correlation 0.8:



Bivariate fractional Brownian motion: Example

For the above bivariate fBm (bfBm) $(B^{(1)}, B^{(2)})^\top$,

$$\text{corr}(\Delta_k B^{(1)}, \Delta_{k-1} B^{(1)}) \approx -.43;$$

$\text{corr}(\Delta_k B^{(2)}, \Delta_{k-1} B^{(2)}) \approx -.14$; $\text{corr}(\Delta_k B^{(2)}, \Delta_{k-1} B^{(1)}) \approx -.24$, such that $B^{(2)}$ is better predictable from the past of $B^{(1)}$ than its own past!

Volatilities exhibit strong co-movements. These can enhance the accuracy of forecasts for individual assets (e.g., multivariate GARCH). In contrast, literature on rough fractional volatility so far restricts to univariate approaches.

↪ modeling and forecasting RV using a multivariate fBm (mfBm) introduced by Amblard et al. (2013) and Coeurjolly et al. (2013).

RMSFE of h -step-ahead forecasts, $h = 1, \dots, 5$, for $B_{(t+h)\Delta}^{(p)}$ based on $n = 500$ recordings:

fBm, $p = 2$.4839	.5044	.5220	.5370	.5492
	(.4802)	(.5077)	(.5254)	(.5387)	(.5495)
bfBm, $p = 2$.4286	.4502	.4698	.4830	.4940
	(.4246)	(.4526)	(.4700)	(.4827)	(.4927)
fBm, $p = 1$.1085	.1420	.1683	.1883	.2067
	(.1085)	(.1430)	(.1681)	(.1886)	(.2061)
bfBm, $p = 1$.0946	.1224	.1441	.1593	.1734
	(.0953)	(.1242)	(.1443)	(.1602)	(.1734)

Outline

- 1 Motivation and literature
- 2 Multivariate fBm and its correlation structure**
- 3 Optimal forecasts for mfBm
- 4 Statistics for mfBm
- 5 Empirical analysis

Multivariate fractional Brownian motion (mfBm)

MfBm is a process $B_t = (B_t^{(1)}, \dots, B_t^{(d)})^\top$, where each component is a fBm with Hurst exponent H_p , $p \in \{1, \dots, d\}$, with covariances for $H_p + H_q \neq 1$:

$$\text{Cov}(B_s^{(p)}, B_t^{(q)}) = \frac{\sigma_p \sigma_q}{2} \left((\rho_{p,q} + \eta_{p,q} \text{sign}(s)) |s|^{H_p+H_q} + (\rho_{p,q} - \eta_{p,q} \text{sign}(t)) |t|^{H_p+H_q} - (\rho_{p,q} - \eta_{p,q} \text{sign}(t-s)) |t-s|^{H_p+H_q} \right).$$

$\rho_{p,q} = \text{corr}(B_1^{(p)}, B_1^{(q)})$ are correlation parameters, while

$$\eta_{p,q} = \frac{\mathbb{E}[B_1^{(p)} B_{-1}^{(q)}] - \mathbb{E}[B_1^{(q)} B_{-1}^{(p)}]}{\sigma_p \sigma_q (2 - 2^{H_p+H_q})}, \text{ if } H_p + H_q \neq 1,$$

with $\eta_{p,q} = -\eta_{q,p}$, are asymmetry parameters.

Time-reversible mfBm: If $\eta_{p,q} = 0$, the covariance simplifies to

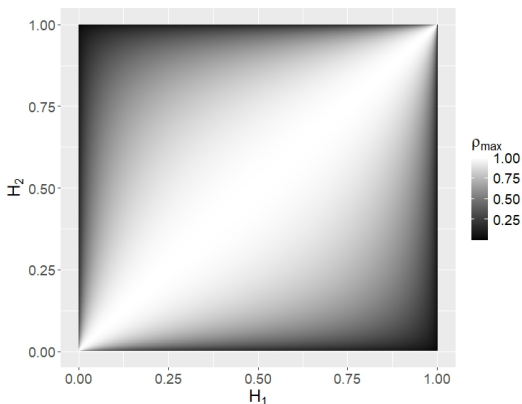
$$\text{Cov}(B_s^{(p)}, B_t^{(q)}) = \frac{\rho_{p,q} \sigma_p \sigma_q}{2} \left(|s|^{2H} + |t|^{2H} - |t-s|^{2H} \right) = \rho_{p,q} \sigma_p \sigma_q w(t, s-t, H),$$

with the cross Hurst exponent $H = (H_p + H_q)/2$.

Maximal possible (absolute) correlation ρ_{max}

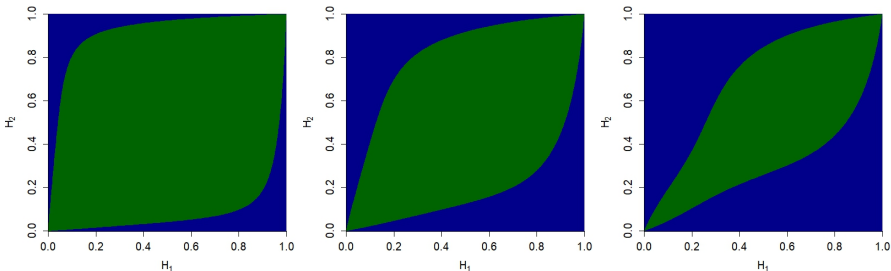
MfBm exists whenever the covariance is positive semi-definite. For time-reversible bfBm with Hurst exponents H_1 and H_2 , this yields a maximal possible (absolute) correlation

$$\rho_{max}(H_1, H_2) = \frac{\sqrt{\sin(\pi H_1) \cdot \sin(\pi H_2) \cdot \Gamma(2H_1 + 1) \cdot \Gamma(2H_2 + 1)}}{\sin(\pi H) \cdot \Gamma(2H + 1)}.$$



Possible parametrizations

For correlations $\rho = 0.5$ (left), $\rho = 0.75$ (middle), and $\rho = 0.9$ (right) each panel shows areas corresponding to the set of (H_1, H_2) for which time-reversible bfBm **exists**, or **does not exist**.



Outline

- 1 Motivation and literature
- 2 Multivariate fBm and its correlation structure
- 3 Optimal forecasts for mfBm**
- 4 Statistics for mfBm
- 5 Empirical analysis

Theoretical insights from simple scenario

For a time-reversible bfBm $(B_t^{(1)}, B_t^{(2)})^\top$, the optimal forecast of $B_{t+h}^{(1)}$, given $B_t^{(1)}, B_t^{(2)}$, is

$$\hat{B}_{t+h|t}^{(1)} = w_{t+h|t}^{11} \cdot B_t^{(1)} + w_{t+h|t}^{12} \cdot B_t^{(2)},$$

for any $\rho \in (-1, 1)$, with weight functions $w_{t+h|t}^{11}$ and

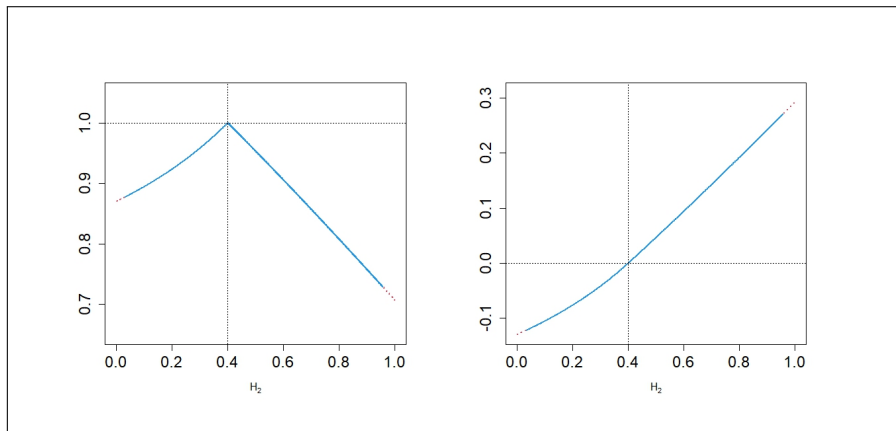
$$w_{t+h|t}^{12} = \frac{\rho}{1 - \rho^2} \frac{\sigma_1}{\sigma_2} \left(\frac{w(t, h, H)}{t^{2H_2}} - \frac{w(t, h, H_1)}{t^{2H}} \right).$$

Its mean squared forecasting error (MSFE) is

$$\begin{aligned} \mathbb{E} \left[\left(\hat{B}_{t+h|t}^{(1)} - B_{t+h|t}^{(1)} \right)^2 \right] &= \sigma_1^2 (t+h)^{2H_1} - \frac{\sigma_1^2}{1 - \rho^2} \frac{(w(t, h, H_1))^2}{t^{2H_1}} \\ &\quad + \frac{\sigma_1^2 \rho^2}{1 - \rho^2} \left(\frac{2w(t, h, H_1)w(t, h, H)}{t^{2H}} - \frac{(w(t, h, H))^2}{t^{2H_2}} \right). \end{aligned}$$

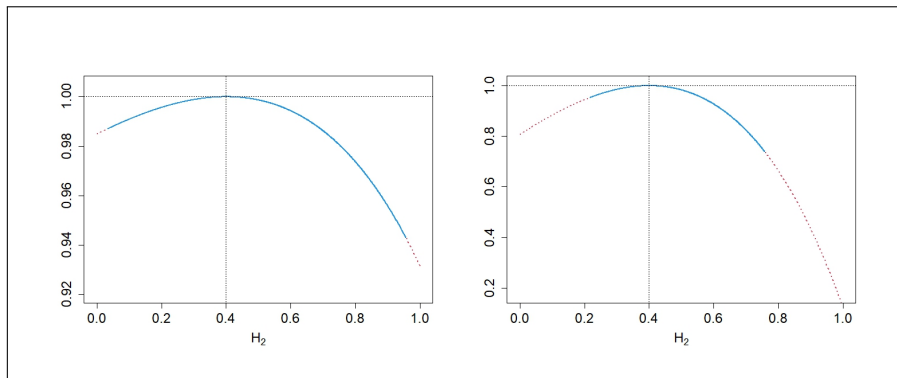
- For $H_1 = H_2$, or $\rho = 0$: $w_{t+h|t}^{12} = 0$, no efficiency gains.
- All other cases result in a **reduced MSFE**.
- Letting $h \downarrow 0$ yields $w_{t+h|t}^{11} \rightarrow 1$ and $w_{t+h|t}^{12} \rightarrow 0$.

Example of forecasting weights for bfBm



Relative weights $w_{2|1}^{11}/(|w_{2|1}^{11}| + |w_{2|1}^{12}|)$ (left) and $w_{2|1}^{12}/(|w_{2|1}^{11}| + |w_{2|1}^{12}|)$ (right), for $\rho = 1/2$, $\sigma_1 = \sigma_2 = 1$ and $H_1 = 0.4$ as functions of H_2 .

Examples of reduced MSFE



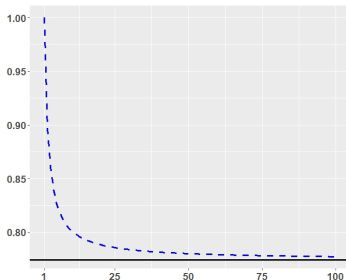
Relative MSFEs for $t = 1$, $h = 1$, $\sigma_1 = \sigma_2 = 1$, as functions of H_2 for $H_1 = 0.4$, with $\rho = 0.5$ (left), and $\rho = 0.9$ (right).

Effect of growing dimension

Conclusions on optimal forecasting drawn from the simple scenario extend similarly to the case of using all historical observations.

What if we go from a bfBm to a mfBm with many components d ?

- MSFE can be further reduced for larger d .
- However, a positive limit exists as $d \rightarrow \infty$.
- Plot: Relative MSFE to univariate one for $t = 10, h = 1, \rho = 0.8, H_1 = 0.1, H = 0.4$.



Outline

- 1 Motivation and literature
- 2 Multivariate fBm and its correlation structure
- 3 Optimal forecasts for mfBm
- 4 Statistics for mfBm**
- 5 Empirical analysis

GMM approach based on acf

Based on autocovariances of increments

$$\text{Cov}(\Delta_k B^{(p)}, \Delta_j B^{(q)}) = \Delta^{H_p+H_q} \sigma_p \sigma_q (\rho_{p,q} \gamma_{p,q}(k-j) + \eta_{p,q} \tilde{\gamma}_{p,q}(k-j)),$$

$$\text{with } \gamma_{p,q}(r) = \frac{1}{2} (|r+1|^{H_p+H_q} + |r-1|^{H_p+H_q} - 2|r|^{H_p+H_q})$$

$$\text{and } \tilde{\gamma}_{p,q}(r) = \frac{1}{2} (\text{sgn}(r+1)|r+1|^{H_p+H_q} + \text{sgn}(r-1)|r-1|^{H_p+H_q} - 2 \text{sgn}(r)|r|^{H_p+H_q}),$$

and of lagged increments $\Delta_{k,\ell_1} B^{(p)} = B_{k\Delta}^{(p)} - B_{(k-\ell_1)\Delta}^{(p)}$:

$$\text{Cov}(\Delta_{k,\ell_1} B^{(p)}, \Delta_{j,\ell_2} B^{(q)}) = \Delta^{H_p+H_q} \sigma_p \sigma_q (\rho_{p,q} \gamma_{p,q}^{\ell_1,\ell_2}(k-j) + \eta_{p,q} \tilde{\gamma}_{p,q}^{\ell_1,\ell_2}(k-j)),$$

$$\text{with } \gamma_{p,q}^{\ell_1,\ell_2}(r) = \frac{1}{2} (|r+\ell_1|^{H_p+H_q} + |r-\ell_2|^{H_p+H_q} - |r|^{H_p+H_q} - |r+\ell_1-\ell_2|^{H_p+H_q})$$

$$\text{and } \tilde{\gamma}_{p,q}^{\ell_1,\ell_2}(r) = \frac{1}{2} (\text{sgn}(r+\ell_1)|r+\ell_1|^{H_p+H_q} + \text{sgn}(r-\ell_2)|r-\ell_2|^{H_p+H_q} - \dots),$$

where $\gamma_{p,q}^{\ell_1,\ell_2}(0) = \ell^{H_p+H_q}$ and $\tilde{\gamma}_{p,q}^{\ell_1,\ell_2}(0) = 0$.

↪ change-of-frequency approach to estimate Hurst exponents.

Parametric inference

Hurst exponents and variances can be component-wise estimated

$$\hat{H}_p = \frac{1}{2 \log(2)} \log \left(\frac{\sum_{k=2}^n (\Delta_{k,2} B^{(p)})^2}{\sum_{k=1}^n (\Delta_k B^{(p)})^2} \right), \quad \hat{\sigma}_p^2 = \frac{\sum_{k=1}^n (\Delta_k B^{(p)})^2}{n \Delta^{2\hat{H}_p}}.$$

Natural pair-wise estimators for correlations and asymmetries:

$$\hat{\rho}_{p,q} = \frac{\sum_{k=1}^n \Delta_k B^{(p)} \cdot \Delta_k B^{(q)}}{\sqrt{\sum_{k=1}^n (\Delta_k B^{(p)})^2 \cdot \sum_{k=1}^n (\Delta_k B^{(q)})^2}},$$

$$\hat{\eta}_{p,q} = \frac{\sum_{k=2}^n (\Delta_{k+1} B^{(q)} \cdot \Delta_k B^{(p)} - \Delta_{k+1} B^{(p)} \cdot \Delta_k B^{(q)})}{\sqrt{\sum_{k=2}^n (\Delta_{k,2} B^{(p)})^2 \sum_{k=2}^n (\Delta_{k,2} B^{(q)})^2 - 2 \sqrt{\sum_{k=1}^n (\Delta_k B^{(p)})^2 \sum_{k=1}^n (\Delta_k B^{(q)})^2}}}.$$

For $\max_p H_p < 3/4$, $H_p + H_q \neq 1$, for all p, q , we prove (feasible) clts with \sqrt{n} rates for these estimators. This yields a consistent asymptotic test for $\eta_{p,q} = 0$ vs. $\eta_{p,q} \neq 0$. An optimal GMM estimator for ρ yields moderate efficiency gains over $\hat{\rho}_{p,q}$.

Parametric inference

Hurst exponents and variances can be component-wise estimated

$$\hat{H}_p = \frac{1}{2 \log(2)} \log \left(\frac{\sum_{k=2}^n (\Delta_{k,2} B^{(p)})^2}{\sum_{k=1}^n (\Delta_k B^{(p)})^2} \right), \quad \hat{\sigma}_p^2 = \frac{\sum_{k=1}^n (\Delta_k B^{(p)})^2}{n \Delta^{2\hat{H}_p}}.$$

Natural pair-wise estimators for correlations and asymmetries:

$$\hat{\rho}_{p,q} = \frac{(\Delta^{H_p+H_q}/n) \sum_{k=1}^n \Delta_k B^{(p)} \cdot \Delta_k B^{(q)}}{\sqrt{(\Delta^{2H_p}/n) \sum_{k=1}^n (\Delta_k B^{(p)})^2 \cdot (\Delta^{2H_q}/n) \sum_{k=1}^n (\Delta_k B^{(q)})^2}},$$

$$\hat{\eta}_{p,q} = \frac{\sum_{k=2}^n (\Delta_{k+1} B^{(q)} \cdot \Delta_k B^{(p)} - \Delta_{k+1} B^{(p)} \cdot \Delta_k B^{(q)})}{\sqrt{\sum_{k=2}^n (\Delta_{k,2} B^{(p)})^2 \sum_{k=2}^n (\Delta_{k,2} B^{(q)})^2 - 2 \sqrt{\sum_{k=1}^n (\Delta_k B^{(p)})^2 \sum_{k=1}^n (\Delta_k B^{(q)})^2}}}.$$

For $\max_p H_p < 3/4$, $H_p + H_q \neq 1$, for all p, q , we prove (feasible) clts with \sqrt{n} rates for these estimators. This yields a consistent asymptotic test for $\eta_{p,q} = 0$ vs. $\eta_{p,q} \neq 0$. An optimal GMM estimator for ρ yields moderate efficiency gains over $\hat{\rho}_{p,q}$.

Multivariate clt for quadratic variation

The normalized discrete **q**uadratic **v**ariation

$$QV_n = \frac{1}{n} \sum_{k=1}^n \begin{pmatrix} \Delta^{-H_1} \Delta_k B^{(1)} \\ \vdots \\ \Delta^{-H_d} \Delta_k B^{(d)} \end{pmatrix} \cdot \begin{pmatrix} \Delta^{-H_1} \Delta_k B^{(1)} \\ \vdots \\ \Delta^{-H_d} \Delta_k B^{(d)} \end{pmatrix}^\top$$

satisfies, with $\Sigma = \text{COV}((B_1^{(1)}, \dots, B_1^{(d)})^\top)$, as $n \rightarrow \infty$, the clt

$$\sqrt{n} \text{vec}(QV_n - \Sigma) \xrightarrow{d} \mathcal{N}\left(0, \sum_{r \in \mathbb{Z}} \Sigma(r)^{\otimes 2} \cdot \mathcal{Z}\right),$$

with (singular) matrix $\mathcal{Z} = \text{COV}(\text{vec}(XX^\top))$, for $X \sim \mathcal{N}(0, I_d)$, and

$$\begin{aligned} (\Sigma(r))_{p,q} &= (\Sigma^s(r))_{p,q} + (\Sigma^a(r))_{p,q} \\ &= \Delta^{H_p+H_q} \sigma_p \sigma_q (\rho_{p,q} \gamma_{p,q}(r) + \eta_{p,q} \tilde{\gamma}_{p,q}(r)). \end{aligned}$$

$D_n \text{vech}(A) = \text{vec}(A)$ is used for reduction. It holds that $\sum_{r \in \mathbb{Z}} \Sigma(r)^{\otimes 2} \cdot \mathcal{Z} = \Sigma^{\otimes 2} \cdot \mathcal{Z} + 2 \sum_{r=1}^{\infty} (\Sigma^s(r)^{\otimes 2} \cdot \mathcal{Z} + \Sigma^a(r)^{\otimes 2} \cdot \tilde{\mathcal{Z}})$, with the duplicated identity $\tilde{\mathcal{Z}} = D_n I_{d^2(d+1)^2/2} D_n^\top$.

How correlations improve inference

Estimate pairwise sum matrix $H \in \mathbb{R}^{d \times d}$, $H_{pq} = H_p + H_q$, $H = H \cdot \mathbf{1}^\top + \mathbf{1} \cdot H$,

$$\hat{H}_{pq} = \frac{1}{\log(2)} \log \left(\frac{(QV_n^{(2)})_{pq}}{(QV_n)_{pq}} \right),$$

with $QV_n^{(2)}$ the normalized discrete lag2-quadratic variation. A joint clt for $(\text{vech}(QV_n)^\top, \text{vech}(QV_n^{(2)})^\top)^\top$, and the Δ -method yield

$$\sqrt{n} \text{vech}(\hat{H} - H) \xrightarrow{d} \mathcal{N}(0, \Sigma_H).$$

Since $\text{vech}(H) = M \cdot H = L_d(I_d \otimes \mathbf{1}^\top + \mathbf{1}^\top \otimes I_d)H$, an optimal estimator

$$\hat{H}_n = (M^\top \Sigma_H^{-1} M)^{-1} M^\top \Sigma_H^{-1} \text{vech}(\hat{H})$$

is of generalized least squares form and satisfies a clt

$$\sqrt{n}(\hat{H}_n - H) \xrightarrow{d} \mathcal{N}(0, (M^\top \Sigma_H^{-1} M)^{-1}).$$

This allows e.g. for an **asymptotic Wald test** for the null $H_1 = \dots = H_d$.

Outline

- 1 Motivation and literature
- 2 Multivariate fBm and its correlation structure
- 3 Optimal forecasts for mfBm
- 4 Statistics for mfBm
- 5 Empirical analysis**

Modeling RVs with mfBM

As Gatheral et al. (2018), Wang et al. (2023), ... model daily log RVs by fBm, but for the first time with mfBm.

Estimated Hurst exponents and correlations across stocks (2005 to 2024).

	H	AAPL	ALD	AMGN	AXP	BA	BEL	CAT	CHV	CRM	CSCO	DIS	GS	HD	IBM	INTC	JNJ	JPM	KO	MCD	MMM		
AAPL	0.2821	1																					
ALD	0.1932	0.39	1																				
AMGN	0.2066	0.37	0.31	1																			
AXP	0.2216	0.38	0.39	0.30	1																		
BA	0.2481	0.38	0.36	0.29	0.36	1																	
BEL	0.1777	0.34	0.33	0.27	0.36	0.27	1																
CAT	0.2050	0.37	0.38	0.24	0.40	0.32	0.30	1															
CHV	0.2196	0.41	0.40	0.31	0.44	0.34	0.39	0.41	1														
CRM	0.2530	0.40	0.31	0.27	0.35	0.28	0.28	0.31	0.33	1													
CSCO	0.2336	0.46	0.39	0.35	0.44	0.37	0.35	0.38	0.46	0.38	1												
DIS	0.2135	0.35	0.32	0.31	0.37	0.30	0.33	0.30	0.39	0.30	0.35	1											
GS	0.2616	0.46	0.41	0.32	0.48	0.39	0.36	0.42	0.45	0.38	0.46	0.42	1										
HD	0.2237	0.41	0.40	0.31	0.36	0.33	0.37	0.34	0.40	0.30	0.41	0.36	0.45	1									
IBM	0.2349	0.39	0.36	0.28	0.35	0.33	0.35	0.36	0.38	0.33	0.40	0.35	0.42	0.35	1								
INTC	0.2247	0.45	0.35	0.32	0.38	0.32	0.32	0.36	0.41	0.35	0.42	0.31	0.40	0.37	0.35	1							
JNJ	0.1363	0.36	0.36	0.32	0.36	0.34	0.39	0.29	0.37	0.31	0.37	0.33	0.45	0.38	0.31	0.31	1						
JPM	0.2326	0.52	0.46	0.35	0.53	0.45	0.45	0.48	0.52	0.39	0.54	0.44	0.68	0.54	0.42	0.45	0.49	1					
KO	0.2122	0.38	0.37	0.29	0.37	0.35	0.39	0.35	0.42	0.32	0.40	0.36	0.44	0.41	0.36	0.36	0.37	0.50	1				
MCD	0.2172	0.35	0.31	0.30	0.32	0.26	0.32	0.32	0.37	0.25	0.33	0.31	0.37	0.39	0.31	0.31	0.31	0.39	0.34	1			
MMM	0.2135	0.35	0.44	0.28	0.40	0.32	0.36	0.44	0.42	0.31	0.39	0.36	0.45	0.39	0.35	0.32	0.41	0.46	0.39	0.34	1		

Empirical analysis: Modeling RVs with mfBM

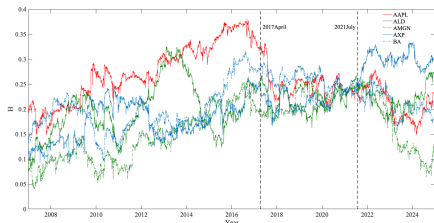
Estimated asymmetries across Dow Jones 30 stocks (2005 to 2024).

	AAPL	ALD	AMGN	AXP	BA	BEL	CAT	CHV	CRM	CSCO	DIS	GS	HD	IBM	INTC	JNJ	JPM	KO	MCD
ALD	0.17																		
AMGN	0.02	-0.12																	
AXP	0.09	-0.18	0.05																
BA	0.11	-0.10	-0.01	-0.02															
BEL	0.17	-0.06	-0.01	-0.02	-0.05														
CAT	0.08	-0.05	0.03	0.00	0.09	-0.02													
CHV	0.13	-0.08	0.10	-0.03	0.01	-0.04	0.01												
CRM	0.09	-0.02	-0.01	-0.05	0.02	-0.05	0.00	0.00											
CSCO	0.21	0.03	0.07	0.06	0.07	-0.02	-0.02	0.04	0.05										
DIS	0.13	-0.09	-0.05	-0.10	-0.07	-0.05	-0.06	-0.14	-0.02	-0.11									
GS	0.11	-0.11	0.02	0.01	0.06	0.02	-0.04	-0.02	0.07	-0.12	0.14								
HD	-0.02	-0.13	-0.06	-0.11	-0.03	-0.13	-0.12	-0.12	-0.08	-0.13	-0.01	-0.06							
IBM	0.02	-0.12	-0.03	-0.11	-0.03	-0.08	-0.00	0.00	-0.02	-0.12	0.04	0.02	0.00						
INTC	0.15	-0.03	0.15	-0.05	0.03	-0.02	-0.01	-0.03	-0.01	0.01	0.14	0.07	0.19	0.05					
JNJ	0.07	-0.07	-0.03	-0.05	-0.00	-0.05	-0.03	-0.07	-0.05	-0.13	-0.05	-0.09	0.03	-0.11	-0.18				
JPM	0.08	-0.09	0.03	0.04	0.09	-0.02	-0.07	0.02	0.01	-0.10	0.08	-0.03	0.04	-0.01	-0.00	0.09			
KO	0.11	-0.04	0.01	-0.06	-0.01	0.00	-0.06	-0.01	-0.01	-0.06	0.15	-0.04	0.06	0.09	-0.04	0.09	0.01		
MCD	0.13	-0.10	-0.03	0.03	-0.01	-0.03	-0.09	-0.02	-0.02	0.06	-0.01	0.00	0.06	-0.03	-0.10	-0.03	0.04	-0.04	
MMM	0.04	-0.08	-0.04	-0.03	-0.01	-0.11	0.10	-0.01	0.03	-0.15	0.11	0.00	0.08	0.03	-0.14	0.08	0.02	-0.08	0.01

The test for time-reversibility does not reject in most cases at a **1% significance level.**

Empirical analysis: Example of forecasting results

Plot: Rolling H estimates for **AAPL** and other assets.



RMSFE of k -day-ahead forecasts for RVs of AAPL with two-year rolling window between

Jan 03, 2007 and Apr 11, 2017:

	$k = 1$	$k = 2$	$k = 5$	$k = 10$
fBm	0.6349	0.8028	1.0137	1.2629
bfBm	0.6328	0.7985	1.0036	1.2474
mfBm3	0.6315	0.7973	0.9998	1.2449
mfBm4	0.6309	0.7970	0.9965	1.2379
mfBm5	0.6301	0.7960	0.9956	1.2378

and Apr 12, 2017 and July 30, 2021:

	$k = 1$	$k = 2$	$k = 5$	$k = 10$
fBm	0.3842	0.5180	0.8080	1.0794
bfBm	0.3849	0.5186	0.8081	1.0782
mfBm3	0.3850	0.5185	0.8081	1.0781
mfBm4	0.3858	0.5191	0.8083	1.0775
mfBm5	0.3855	0.5191	0.8090	1.0793

Forecasts based on mfBm significantly improve when Hurst exponents differ.

Empirical analysis: Example of forecasting results

More empirical findings:

- Forecasts clearly **outperform time series benchmark methods**.
- Analogous results using **QLIKE** as loss function.
- **Vector HAR model fails to improve forecasting accuracy**.
 \rightsquigarrow multivariate models do not necessarily yield efficiency gains.
- **Model confidence sets** underscore advantage of mfBm.

RMSFE of k -day-ahead forecasts for RVs of AAPL with two-year rolling window between

Apr 12, 2017 and Jan 14, 2025:

	$k = 1$	$k = 2$	$k = 5$	$k = 10$
fBm	0.5003	0.6428	0.8523	1.0705
bfBm	0.4993	0.6405	0.8465	1.0611
mfBm3	0.4986	0.6397	0.8439	1.0592
mfBm4	0.4984	0.6397	0.8419	1.0548
mfBm5	0.4979	0.6391	0.8415	1.0550

compared to the vector HAR model¹:

	$k = 1$	$k = 2$	$k = 5$	$k = 10$
HAR	0.5157	0.6513	0.8678	1.1109
VHAR2	0.5316	0.6703	0.9307	1.2834
VHAR3	0.5384	0.6838	0.9563	1.3236
VHAR4	0.5457	0.6977	0.9852	1.3666
VHAR5	0.5580	0.7072	1.0088	1.3626

¹Ding, Y., Engle, R., Li, Y. and Zheng, X. (2025). Multiplicative factor model for volatility. *Journal of Econometrics* 249, 105959.

Ongoing and future research

Next steps:

- Extend the theory from model ① to model ②.
- In independent research, Dugo et al.² construct a **multivariate fOU process** as volatility model. Differences should be considered in high- and low-frequency regime.
- Introduce **mmfBm**, and apply it for a **change-point analysis**.
- Forecasting with asymmetries.
- As **mixed fBm** is a natural model for signed order flow;³ more statistical theory and multivariate extensions remain to be developed.
- FBm is only used for volatilities. Multivariate settings call for fractional **co-volatility matrix models**.

²Ranieri Dugo, Giacomo Giorgio and Paolo Pigato (2026). The multivariate fractional Ornstein-Uhlenbeck process. *Stochastic Processes and their Applications* 192, 104814.

³Muhle-Karbe, J., Chahdi, Y.O., Rosenbaum, M., and Szymanski, G. (2026+). A unified theory of order flow, market impact, and volatility, arxiv: 2601.23172

References

Amblard, P.-O. and Coeurjolly, J.-F. (2011). Identification of the multivariate fractional Brownian motion. *IEEE Transactions on Signal Processing*, 59(11):5152–5168.

Amblard, P.-O., Coeurjolly, J.-F., Lavancier, F., and Philippe, A. (2013). Basic properties of the multivariate fractional Brownian motion. In *Séminaires et congrès, volume 28*, pages 65–87.

Bibinger, M., Yu, J., Zhang, C. (2025+). Modeling and Forecasting Multivariate Realized Volatility with Multivariate Fractional Brownian Motion. *preprint, arxiv: 2504.15985*

Fukasawa, M., Takabatake, T., and Westphal, R. (2022). Consistent estimation for fractional stochastic volatility model under high-frequency asymptotics. *Mathematical Finance* 32(4), 1086–1132.

Gatheral, J., Jaisson, T., and Rosenbaum, M. (2018). Volatility is rough. *Quantitative Finance*, 18(6):933–949.

Wang, X., Xiao, W., and Yu, J. (2023). Modeling and forecasting realized volatility with the fractional Ornstein–Uhlenbeck process. *Journal of Econometrics*, 232(2):389–415.

Thank you for your attention.